

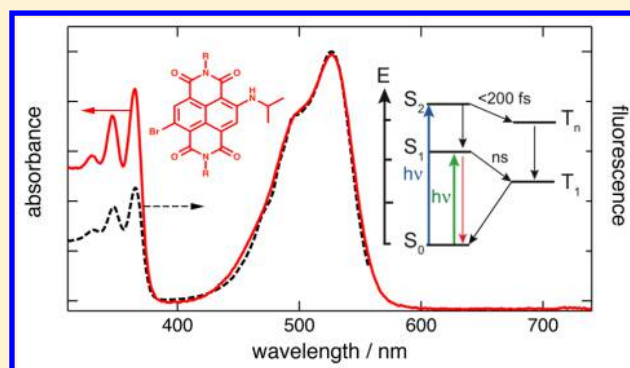
# Ultrafast Intersystem-Crossing Dynamics and Breakdown of the Kasha–Vavilov’s Rule of Naphthalenediimides

Oleksandr Yushchenko, Giuseppe Licari, Sandra Mosquera-Vazquez, Naomi Sakai, Stefan Matile, and Eric Vauthey\*

School of Chemistry and Biochemistry, University of Geneva, 30 Quai Ernest Ansermet, Geneva 4 CH-1211, Switzerland

**S** Supporting Information

**ABSTRACT:** The fluorescence quantum yield of a red naphthalenediimide dye (rNDI) with amino and Br core substituents has been found to decrease by a factor of almost 2 by going from  $S_1 \leftarrow S_0$  to  $S_2 \leftarrow S_0$  excitation. Time-resolved spectroscopic measurements reveal that this deviation from the Kasha–Vavilov’s rule is due to an ultrafast, < 200 fs, intersystem-crossing (ISC) from the  $S_2$  state to the triplet manifold, due to the  $\pi\pi^* \rightarrow n\pi^*$  character of the transition and to the presence of the heavy Br atom. In non-core substituted naphthalenediimide (pNDI), ISC is slower,  $\sim 2$  ps, and was found to be reversible on a time scale shorter than that of vibrational cooling. The fluorescence and triplet quantum yields of rNDI, thus, can be substantially changed by a simple variation of the excitation wavelength.



One of the most important rules in organic photophysics and photochemistry is the Kasha–Vavilov’s rule that states that emission takes place from the lowest electronic excited state, namely the  $S_1$  and  $T_1$  states for closed-shell molecules, and that the emission quantum yields do not depend on the excitation wavelength.<sup>1</sup> This rule finds its basis in the ultrashort lifetime of upper electronic excited states, which originates from highly efficient internal conversion to nearby states of the same multiplicity and from very fast intra- and intermolecular vibrational relaxation.<sup>2</sup> Unless photoionization processes or multichromophoric systems are considered, the exceptions to this rule are scarce.<sup>3–16</sup>

We present here our investigation of the photophysics of a red core-substituted naphthalenediimide dye, r(ed)NDI (Figure 1), whose fluorescence quantum yield decreases by a factor of almost two when exciting the  $S_2 \leftarrow S_0$  instead of the  $S_1 \leftarrow S_0$  transition. We will show that this departure from the Kasha–Vavilov’s rule is due to an ultrafast intersystem crossing (ISC) from the  $S_2$  state to the triplet manifold that competes with internal conversion to the  $S_1$  state. For the past few years, these core-substituted naphthalenediimides (c-NDIs) have been intensively used as building blocks in the elaboration of sophisticated molecular architectures developed for various applications, such as photovoltaics, artificial photosynthesis, or sensing.<sup>17–24</sup> Contrary to the non-core-substituted naphthalenediimides (NDIs) that are colorless and barely fluorescent,<sup>25–28</sup> c-NDIs absorb in the visible and exhibit fluorescence with quantum yields  $\Phi_f$  that are typically larger than 0.1. This difference is due to the nature of the  $S_1 \leftarrow S_0$  transition, which involves a substantial redistribution of the electronic density

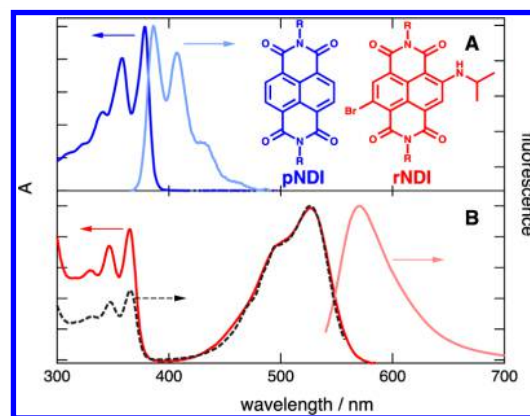


**Figure 1.** Absorption and fluorescence spectra of pNDI (A) and rNDI (B) in ACN. The fluorescence excitation spectrum of rNDI is also shown in B (dashed line). The complete structures of pNDI and rNDI are given in Supporting Information Scheme S1.

from the core substituents to the carbonyl groups. As a consequence, the energy of this state as well as the redox properties of c-NDIs can be tuned by varying the electron-donating ability of the substituents.

As the  $S_2 \leftarrow S_0$  transition of c-NDIs hardly involves the core substituents, the  $S_2$  state resembles the  $S_1$  state of the conventional NDIs. Therefore, in order to better understand

Received: April 28, 2015

Accepted: May 19, 2015

Published: May 19, 2015

the excited-state dynamics of rNDI upon  $S_2 \leftarrow S_0$  excitation, we have also investigated that of a NDI without core substituents, p(ale)NDI (Figure 1). Although these NDIs are being very intensively used as acceptors in electron-transfer cascades,<sup>29–35</sup> their excited-state dynamics, especially those of the ultrafast ISC from the  $S_1$  state responsible for the negligible fluorescence, have not been investigated in much detail. The fluorescence lifetime of NDIs with different imide substituents has been estimated to be in the 5–20 ps range.<sup>27,28</sup> More recently, Ganesan et al. performed femtosecond transient absorption measurements of pNDI in chloroform and reported an ISC time constant of 10 ps.<sup>36</sup> We will show here that the ISC dynamics from the  $S_1$  state of pNDI to the triplet manifold is more complex than previously assumed.

Figure 1 shows the absorption and fluorescence spectra of pNDI and rNDI in acetonitrile (ACN). Whereas the spectrum of pNDI exhibits the characteristic structured band of naphthalenediimides below 400 nm, that of rNDI contains a similar band shifted by  $940\text{ cm}^{-1}$  to higher energy, which corresponds to the  $S_2 \leftarrow S_0$  transition, as well as the  $S_1 \leftarrow S_0$  band at 528 nm, which involves the core substituents. Similarly to other NDIs with different imide substituents,<sup>25,27,28,36,37</sup> pNDI is hardly fluorescent with  $\Phi_{\text{fl}} \sim 10^{-3}$ , whereas rNDI shows intense fluorescence around 570 nm with  $\Phi_{\text{fl}} = 0.22$  in ACN upon  $S_1 \leftarrow S_0$  excitation. However, as illustrated by its excitation spectrum (Figure 1B), rNDI departs from the Kasha–Vavilov’s rule as its fluorescence quantum yield decreases by a factor of 1.9 upon  $S_2 \leftarrow S_0$  excitation. As the fluorescence lifetime of rNDI amounts to 5.5 ns independently of the excitation wavelength (375 or 470 nm), this decrease of  $\Phi_{\text{fl}}$  should arise from the existence of a relaxation pathway of the  $S_2$  state that competes with internal conversion to the  $S_1$  state.

Further insight into the origin of this breaking of the Kasha–Vavilov’s rule was obtained by comparing the transient absorption (TA) spectra measured with rNDI upon  $S_1 \leftarrow S_0$  excitation at 532 nm and  $S_2 \leftarrow S_0$  excitation at 385 and 355 nm in ACN (Figure 2) and in dichloromethane (DCM, Supporting Information Figure S1–S2).<sup>38,39</sup> The TA spectra recorded within the first nanosecond after 532 nm excitation are dominated by a positive band extending from 370 to 510 nm that can be assigned to  $S_n \leftarrow S_1$  absorption, and by negative bands at 365 nm and in the 540–650 nm region that are due to ground-state bleach and stimulated emission, respectively.<sup>40</sup> During the next  $\sim 10$  ns, the positive band transforms into a band peaking at 440 nm, and the stimulated emission is replaced by a positive absorption band. In ACN, this spectrum decays on the  $\sim 1\text{ }\mu\text{s}$  time scale to a weak residual spectrum with two bands around 450 and 600 nm, which itself decays to zero within 10  $\mu\text{s}$ . In DCM, the spectrum with the 440 nm band decays entirely to zero, and no residual spectrum is observed (Supporting Information Figure S1). Global analysis using the sum of three exponential functions or target analysis assuming three sequential steps (A  $\rightarrow$  B  $\rightarrow$  C  $\rightarrow$  D) could successfully reproduce the TA data in ACN with the time constants and species-associated difference spectra (SADS) shown in Figure 2C.<sup>41</sup> The first step with a time constant identical to the fluorescence lifetime can be assigned to the decay of the  $S_1$  state population to the ground state and to the triplet state (species B) by ISC. The second step (B  $\rightarrow$  C) can be interpreted as the decay of the triplet-state population to the ground state and to another state (species C), which is only present in ACN. Assignment of B to the triplet state of rNDI is

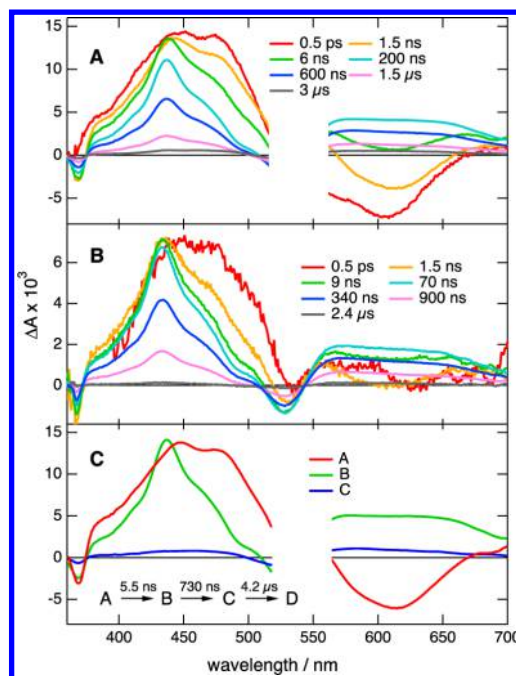


**Figure 2.** Transient absorption spectra recorded at several time delays after (A)  $S_1 \leftarrow S_0$  and (B)  $S_2 \leftarrow S_0$  excitation of rNDI in ACN and (C) species-associated difference spectra obtained from target analysis of the spectra shown in (A) assuming the scheme in the inset.

comforted by a shortening of its lifetime in aerated solutions. As the SADS of C resembles strongly the absorption spectrum of the radical anion of an analogue of rNDI with a Cl atom instead of the Br substituent,<sup>40</sup> C is interpreted as  $\text{rNDI}^{\cdot-}$ . This ion most probably results from triplet–triplet annihilation, as already reported for several organic ketones in polar solvents.<sup>42</sup> The cation  $\text{rNDI}^{\cdot+}$  should also be generated during this process. However, the Cl analogue of  $\text{rNDI}^{\cdot+}$  has been shown to have either a very similar absorption spectrum as that of the anion or a weak absorption in the visible.<sup>40</sup> Previous observations of photoinduced symmetry-breaking charge separation (SB-CS) between other c-NDIs support the formation of ions by triplet–triplet annihilation in polar solvents.<sup>22,40,43</sup> According to the redox potentials of rNDI,<sup>21</sup> this process should be energetically feasible in ACN, but not in DCM (see Supporting Information), in agreement with our observation.

The TA spectra recorded during the first few nanoseconds after  $S_2 \leftarrow S_0$  excitation show several differences (Figure 2B): (1) the 440 nm band dominates at much earlier time and (2) the stimulated emission band is barely visible. On the other hand, the spectra recorded after  $\sim 10$  ns are mostly identical to those obtained upon 532 nm excitation and can be assigned to the  $T_1$  population. The same target analysis yields similar time constants and SADS for B and C. However, as shown in Supporting Information Figure S3A, the SADS obtained for A contains features of both  $S_1$  and  $T_1$  spectra, indicating that the  $T_1$  state contributes to this SADS as well. Target analysis assuming that both the  $S_1$  and  $T_1$  states are initially equally populated (i.e.,  $A(0) = B(0) = 0.5$ ) yields SADS, which are identical to those obtained above from the 532 nm TA data (compare Figure 2C with Supporting Information Figure S3B). Thus, these results are fully consistent with the reduced fluorescence quantum yield measured upon  $S_2 \leftarrow S_0$  excitation and points to the occurrence of an ultrafast ISC process from

the  $S_2$  state to the triplet manifold that competes with internal conversion. According to the TA data, the decay of the  $S_2$  state takes place within the instrument response, that is, around 200 fs.

To better understand how core substitution affects the ISC dynamics of rNDI  $S_2$  state, TA measurements have also been performed with pNDI in the same two solvents (Figure 3 and

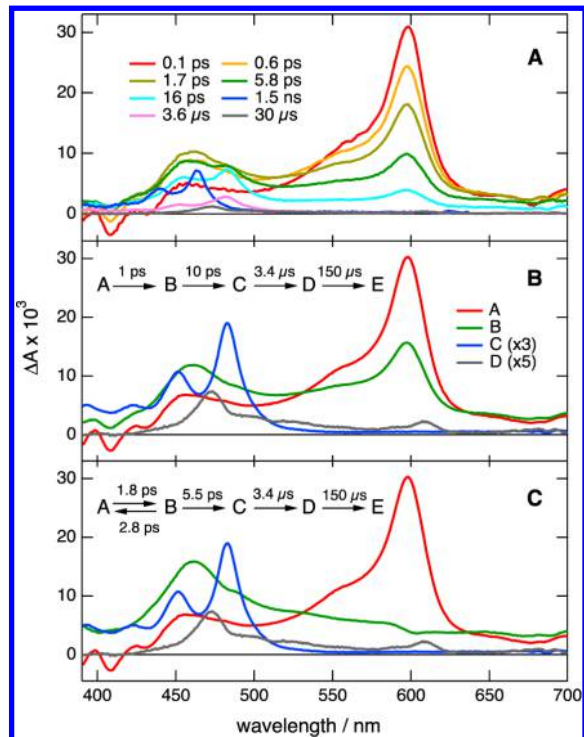


**Figure 3.** (A) Transient absorption spectra recorded at several time delays after  $S_1 \leftarrow S_0$  excitation of pNDI in ACN and (B),(C) species-associated difference spectra obtained from target analysis assuming the reaction scheme in the inset.

Supporting Information Figure S4). The TA spectra are first dominated by a band at 597 nm, which loses half of its intensity after only 2 ps, whereas another weaker band rises at 460 nm. Afterward, both bands decay simultaneously within a few tens of picoseconds and a structured band with the maximum at 483 nm rises. In DCM (Supporting Information Figure S4), this band decreases entirely to zero on the microsecond time scale. In ACN, it transforms into a spectrum with bands at 473 and 608 nm, which lives for hundreds of microseconds.

Target analysis assuming sequential steps yields the time constants and SADS shown in Figure 3B and Supporting Information Figure S4B. Species C can be undoubtedly assigned to the  $T_1$  state of pNDI,<sup>36,44</sup> whereas species D is attributed to pNDI<sup>-</sup> because its spectrum is essentially the same as that of the radical anion of a similar NDI.<sup>45</sup> pNDI<sup>-</sup> is most probably generated by SB-CS upon triplet–triplet annihilation as discussed above with rNDI. Whereas species A can be safely assigned to the  $S_1$  state of pNDI, the interpretation of SADS B is not evident as it also contains the 597 nm band. The fluorescence decays of pNDI measured at several wavelengths between 420 and 450 nm are biexponential with the same time constants, that is, 1 and 10 ps, as found for the  $A \rightarrow B \rightarrow C$  steps (Supporting Information Figure S5). As their associated amplitudes do not depend on the emission wavelength, these time constants are not due to solvent/

vibrational relaxation or two different emitting states. The B SADS suggests the decay of two different states/species with the same time constant. All this can be accounted for by an equilibrium between the  $S_1$  state and species B. The result of a target analysis of the TA data with a scheme including such an equilibrium is shown in Figure 3C. The SADS of A and B are now totally different and thus arise from distinct species/states. Because of this equilibrium, the decay of the  $S_1$  state is now biexponential, in agreement with the fluorescence measurements. Previous investigations on related NDIs pointed to the presence of an upper excited triplet state with  $n\pi^*$  character close to the  $S_1 \pi\pi^*$  state.<sup>28</sup> This is confirmed by quantum chemistry calculations that predict a triplet state,  $T_4$ , with  $n\pi^*$  character at the same energy as the  $S_1$  state (Supporting Information Table S1). This suggests that species B is this  $T_4$  state, and that back-ISC to the  $S_1$  state competes with internal conversion to lower triplet states (Figure 4). The latter process

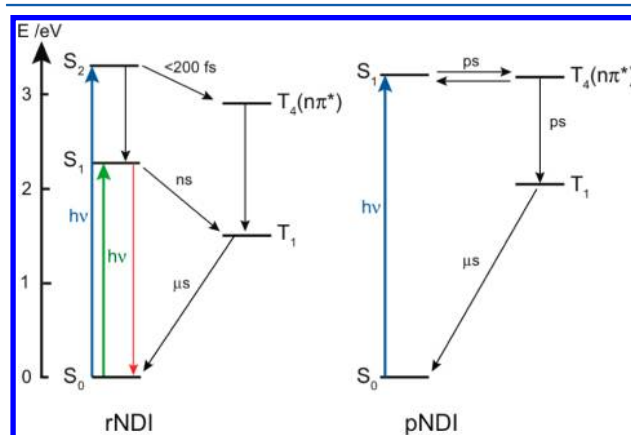


**Figure 4.** Energy level scheme of rNDI and pNDI with the most relevant relaxation pathways and time scale (unless specified, the excited states have a  $\pi\pi^*$  character, intermolecular processes have been omitted).

requires the release of a substantial amount of energy into the environment, a process that occurs on a few picoseconds time scale,<sup>46,47</sup> in good agreement with the 3–5 ps time constant for the  $T_4 \rightarrow T_1$  process obtained from target analysis.

The above results reveal that ISC to the triplet manifold occurs with a 2 ps time constant in pNDI. As a consequence, the much faster ISC from the  $S_2$  state measured with rNDI should be related to the core substituents. According to quantum chemistry calculations, the only available triplet state of  $n\pi^*$  character is  $T_4$  and is located 0.4 eV below  $S_2$  (Supporting Information Table S2). This larger singlet–triplet energy gap compared to pNDI explains the absence of back-ISC with rNDI, but should not accelerate  $S_2 \rightarrow T_4$  ISC. The key factor responsible for the faster ISC of rNDI and, thus, the breakdown of the Kasha–Vavilov’s rule is the presence of the Br core substituent, which further increases the spin–orbit coupling associated with the  $S_2(\pi\pi^*) \rightarrow T_4(n\pi^*)$  transition<sup>48</sup> and makes ISC as fast as  $S_2 \rightarrow S_1$  internal conversion (Figure 4). This is confirmed by fluorescence excitation spectra measured with other c-NDIs that do not have heavy core substituents and do not exhibit any deviation from the Kasha–Vavilov’s rule (Supporting Information Figure S6). This sub-200-fs ISC from rNDI is among the fastest reported for an organic molecule.

Whereas c-NDIs are already valued for the high tunability of their optical and electrochemical properties upon modest chemical modification, the results presented here reveal a new facet of their versatility, namely the possibility to influence their excited-state dynamics by varying the magnitude of the spin-orbit coupling. This allows the design of dyes like rNDI, whose fluorescence and triplet quantum yields be substantially changed by a simple variation of the excitation wavelength.

## ■ ASSOCIATED CONTENT

### ■ Supporting Information

Synthesis of rNDI and pNDI, experimental details, calculations of the driving force for symmetry-breaking charge separation, transient absorption data in DCM, time-resolved fluorescence, electronic absorption spectra of other c-NDIs, and quantum chemical calculations. The Supporting Information is available free of charge on the ACS Publications website at DOI: 10.1021/acs.jpcllett.5b00882.

## ■ AUTHOR INFORMATION

### Corresponding Author

\*E-mail: eric.vauthey@unige.ch.

### Notes

The authors declare no competing financial interest.

## ■ ACKNOWLEDGMENTS

This work was supported by the Swiss National Science Foundation through project no. 200020-147098 and 200020-150000, and the University of Geneva, the European Research Council (ERC Advanced Investigator), the National Centre of Competence in Research (NCCR) Chemical Biology and the NCCR Molecular Systems Engineering.

## ■ REFERENCES

- (1) Turro, N. J.; Ramamurthy, V.; Scaiano, J. C. *Modern Molecular Photochemistry of Organic Molecules*; University Science Books: Sausalito, CA, 2010.
- (2) Rosspeintner, A.; Lang, B.; Vauthey, E. Ultrafast Photochemistry in Liquids. *Annu. Rev. Phys. Chem.* **2013**, *64*, 247–271.
- (3) Longuet-Higgins, H. C.; Beer, M. Anomalous Light Emission of Azulene. *J. Chem. Phys.* **1955**, *23*, 1390.
- (4) Maciejewski, A.; Steer, R. P. The Photophysics, Physical Chemistry and Related Spectroscopy of Thiocarbonyls. *Chem. Rev.* **1993**, *93*, 67–98.
- (5) Itoh, T. Low-Lying Electronic States, Spectroscopy, and Photophysics of Linear Para Acenquinones. *Chem. Rev.* **1995**, *95*, 2351–2368.
- (6) Itoh, T. Fluorescence and Phosphorescence from Higher Excited States of Organic Molecules. *Chem. Rev.* **2012**, *112*, 4541–4568.
- (7) Bajema, L.; Gouterman, M.; Rose, C. B. Porphyrins XXIII: Fluorescence of the Second Excited Singlet and Quasiline Structure of Zinc Tetrabenzoporphin. *J. Mol. Spectrosc.* **1971**, *39*, 421–428.
- (8) Gurzadyan, G. G.; Tran-Thi, T.-H.; Gustavsson, T. Time-Resolved Fluorescence Spectroscopy of High-Lying Electronic States of Zn-Tetraphenylporphyrin. *J. Chem. Phys.* **1998**, *108*, 385–388.
- (9) Mazurak, Z.; Wanic, A.; Karolczak, J.; Czaja, M. The Fluorescence Decay Times and Quantum Efficiencies of 1,4,5,8-Naphthalisoimides. *J. Lumin.* **2015**, *158*, 103–109.
- (10) Henry, K. E.; Balasingham, R. G.; Vortherms, A. R.; Platts, J. A.; Valliant, J. F.; Coogan, M. P.; Zubietta, J.; Doyle, R. P. Emission Wavelength Variation with Changes in Excitation in a Re(i)-bisthiazole Ligand Complex that Breaks the Kasha–Vavilov Rule. *Chem. Sci.* **2013**, *4*, 2490–2495.
- (11) Barbařina, A.; Latterini, L.; Carloti, B.; Elisei, F. Characterization of Excited States of Quinones and Identification of Their Deactivation Pathways. *J. Phys. Chem. A* **2010**, *114*, 5980–5984.
- (12) Lavi, A.; Johnson, F. M.; Ehrenberg, B. Wavelength Dependence of the Fluorescence and Singlet Oxygen Quantum Yields of New Photosensitizers. *Chem. Phys. Lett.* **1994**, *231*, 144–150.
- (13) Callomon, J. H.; Parkin, J. E.; Lopez-Delgado, R. Non-Radiative Relaxation of the Excited  $\bar{A}$  1B<sub>2u</sub> State of Benzene. *Chem. Phys. Lett.* **1972**, *13*, 125–131.
- (14) Féraud, G.; Pino, T.; Falvo, C.; Parneix, P.; Combriat, T.; Bréchnignac, P. Intramolecular Processes Revealed Using UV-Laser-Induced IR-Fluorescence: A New Perspective on the “Channel Three” of Benzene. *J. Phys. Chem. Lett.* **2014**, *5*, 1083–1090.
- (15) Liu, Y.; Knopp, G.; Hemberger, P.; Sych, Y.; Radi, P.; Bodi, A.; Gerber, T. Ultrafast Imaging of Electronic Relaxation in o-Xylene: a New Competing Intersystem Crossing Channel. *Phys. Chem. Chem. Phys.* **2013**, *15*, 18101–18107.
- (16) Brodard, P.; Sarbach, A.; Gumy, J.-C.; Bally, T.; Vauthey, E. Excited State Dynamics of Organic Radical Ions in Liquids and in Low-Temperature Matrices. *J. Phys. Chem. A* **2001**, *105*, 6594–6601.
- (17) Würthner, F.; Shahadat, A.; Thalacker, C.; Debaerdemaeker, T. Core-Substituted Naphthalene Bisimides: New Fluorophors with Tunable Emission Wavelength for FRET Studies. *Chem.—Eur. J.* **2002**, *8*, 4742.
- (18) Röger, C.; Würthner, F. Core-Tetrasubstituted Naphthalene Diimides: Synthesis, Optical Properties, and Redox Characteristics. *J. Org. Chem.* **2007**, *72*, 8070–8075.
- (19) Bhosale, S. V.; Bhosale, S. V.; Kalyankar, M. B.; Langford, S. J. A Core-Substituted Naphthalene Diimide Fluoride Sensor. *Org. Lett.* **2009**, *11*, 5418–5421.
- (20) Villamaina, D.; Kelson, M. M. A.; Bhosale, S. V.; Vauthey, E. Excitation Wavelength Dependence of the Charge Separation Pathways in Tetraporphyrin–Naphthalene Diimide Pentads. *Phys. Chem. Chem. Phys.* **2014**, *16*, 5188–5200.
- (21) Sakai, N.; Mareda, J.; Vauthey, E.; Matile, S. Core-Substituted Naphthalenediimides. *Chem. Commun.* **2010**, *46*, 4225–4237.
- (22) Sakai, N.; Lista, M.; Kel, O.; Sakurai, S.-i.; Emery, D.; Mareda, J.; Vauthey, E.; Matile, S. Self-Organizing Surface-Initiated Polymerization: Facile Access to Complex Functional Systems. *J. Am. Chem. Soc.* **2011**, *133*, 15224–15227.
- (23) Sisson, A. L.; Sakai, N.; Banerji, N.; Fürstenberg, A.; Vauthey, E.; Matile, S. Zipper Assembly of Vectorial Rigid-Rod-Stack Architectures with Red and Blue Naphthalenediimides: Toward Supramolecular Cascade n/p-Heterojunctions. *Angew. Chem., Int. Ed.* **2008**, *47*, 3727–3729.
- (24) Bhosale, S.; Sisson, A. L.; Talukdar, P.; Fürstenberg, A.; Banerji, N.; Vauthey, E.; Bollot, G.; Mareda, J.; Röger, C.; Würthner, F.; et al. Photoproduction of Proton Gradients with Pi-Stacked Fluorophore Scaffolds in Lipid Bilayers. *Science* **2006**, *313*, 84–86.
- (25) Barros, T. C.; Brochsztain, S.; Toscano, V. G.; Berci Filho, P.; Politi, M. J. Photophysical Characterization of a 1,4,5,8-Naphthalenediimide Derivative. *J. Photochem. Photobiol., A* **1997**, *111*, 97–104.
- (26) Refat, M. S.; Grabchev, I.; Chovelon, J. M.; Ivanova, G. Spectral Properties of New N,N'-bis-Alkyl-1,4,6,8-naphthalenediimide Complexes. *Spectrochim. Acta, Part A* **2006**, *64A*, 435–441.
- (27) Alp, S.; Erten, S.; Karapire, C.; Koz, B.; Doroshenko, A. O.; Icli, S. Photoinduced Energy-Electron Transfer Studies with Naphthalene Diimides. *J. Photochem. Photobiol., A* **2000**, *135*, 103–110.
- (28) Wintgens, V.; Valat, P.; Kossanyi, J.; Biczok, L.; Demeter, A.; Berces, T. Spectroscopic Properties of Aromatic Dicarboximides. *J. Chem. Soc. Faraday Trans.* **1994**, *90*, 411.
- (29) Borgström, M.; Shaikh, N.; Johansson, O.; Anderlund, M. F.; Styring, S.; Aakermark, B.; Magnuson, A.; Hammarström, L. Light Induced Manganese Oxidation and Long-Lived Charge Separation in a Mn<sup>2+</sup>-Ru<sup>II</sup>(bpy)<sub>3</sub>-Acceptor Triad. *J. Am. Chem. Soc.* **2005**, *127*, 17504–17515.
- (30) Pellegrin, Y.; Odobel, F. Molecular Devices Featuring Sequential Photoinduced Charge Separations for the Storage of Multiple Redox Equivalents. *Coord. Chem. Rev.* **2011**, *255*, 2578–2593.

(31) Sazanovich, I. V.; Alamiry, M. A. H.; Best, J.; Bennett, R. D.; Bouganov, O. V.; Davies, E. S.; Grivin, V. P.; Meijer, A. J. H. M.; Plyusnin, V. F.; Ronayne, K. L.; et al. Excited State Dynamics of a Pt<sup>II</sup> Diimine Complex Bearing a Naphthalene-Diimide Electron Acceptor. *Inorg. Chem.* **2008**, *47*, 10432–10445.

(32) Ghiggino, K. P.; Hutchison, J. A.; Langford, S. J.; Latter, M. J.; Lee, M. A. P.; Lowenstern, P. R.; Scholes, C.; Takezaki, M.; Wilman, B. E. Porphyrin-Based Molecular Rotors As Fluorescent Probes of Nanoscale Environments. *Adv. Funct. Mater.* **2007**, *17*, 805–813.

(33) Guo, X.; Gan, Z.; Luo, H.; Araki, Y.; Zhang, D.; Zhu, D.; Ito, O. Photoinduced Electron-Transfer Processes of Tetrathiafulvalene-(Spacer)-(Naphthalenediimide)-(Spacer)-Tetrathiafulvalene Triads in Solution. *J. Phys. Chem. A* **2003**, *107*, 9747–9753.

(34) Miller, S. E.; Lukas, A. S.; Marsh, E.; Bushard, P.; Wasielewski, M. R. Photoinduced Charge Separation Involving an Unusual Double Electron Transfer Mechanism in a Donor-Bridge-Acceptor Molecule. *J. Am. Chem. Soc.* **2000**, *122*, 7802–7810.

(35) Greenfield, S. R.; Svec, W. A.; Gosztola, D.; Wasielewski, M. R. Multistep Photochemical Charge Separation in Rod-Like Molecules Based on Aromatic Imides and Diimides. *J. Am. Chem. Soc.* **1996**, *118*, 6767–6777.

(36) Ganesan, P.; Baggerman, J.; Zhang, H.; Sudholter, E. J. R.; Zuilhof, H. Femtosecond Time-Resolved Photophysics of 1,4,5,8-Naphthalene Diimides. *J. Phys. Chem. A* **2007**, *111*, 6151–6156.

(37) Abraham, B.; McMasters, S.; Mullan, M. A.; Kelly, L. A. Reactivities of Carboxyalkyl-Substituted 1,4,5,8-Naphthalene Diimides in Aqueous Solution. *J. Am. Chem. Soc.* **2004**, *126*, 4293–4300.

(38) Banerji, N.; Duvanel, G.; Perez-Velasco, A.; Maity, S.; Sakai, N.; Matile, S.; Vauthey, E. Excited-State Dynamics of Hybrid Multichromophoric Systems: Toward an Excitation Wavelength Control of the Charge Separation Pathways. *J. Phys. Chem. A* **2009**, *113*, 8202–8212.

(39) Lang, B.; Mosquera-Vazquez, S.; Lovy, D.; Sherin, P.; Markovic, V.; Vauthey, E. Broadband Ultraviolet-Visible Transient Absorption Spectroscopy in the Nanosecond to Microsecond Time Domain with Sub-Nanosecond Time Resolution. *Rev. Sci. Instrum.* **2013**, *84*, 073107–8.

(40) Banerji, N.; Fürstenberg, A.; Bhosale, S.; Sisson, A. L.; Sakai, N.; Matile, S.; Vauthey, E. Ultrafast Photoinduced Charge Separation in Naphthalene Diimide Based Multichromophoric Systems in Liquid Solutions and in a Lipid Membrane. *J. Phys. Chem. B* **2008**, *112*, 8912–8922.

(41) van Stokkum, I. H. M.; Larsen, D. S.; van Grondelle, R. Global and Target Analysis of Time-Resolved Spectra. *Biochim. Biophys. Acta, Bioenerg.* **2004**, *1657*, 82–104.

(42) Jacques, P.; Allonas, X.; Sarbach, A.; Haselbach, E.; Vauthey, E. Tuning the Ion Formation Processes from Triplet–Triplet Annihilation to Triplet Mediated Photoionisation. *Chem. Phys. Lett.* **2003**, *378*, 185.

(43) Vauthey, E. Photoinduced Symmetry-Breaking Charge Separation. *ChemPhysChem* **2012**, *13*, 2001–2011.

(44) Green, S.; Fox, M. A. Intramolecular Photoinduced Electron Transfer from Nitroxyl Radicals. *J. Phys. Chem.* **1995**, *99*, 14752–14757.

(45) Gosztola, D.; Niemczik, M. P.; Svec, W.; Lukas, A. S.; Wasielewski, M. R. Excited Doublet States of Electrochemically Generated Aromatic Imide and Diimide Radical Anions. *J. Phys. Chem. A* **2000**, *104*, 6545–6551.

(46) Pigliucci, A.; Duvanel, G.; Daku, L. M. L.; Vauthey, E. Investigation of the Influence of Solute–Solvent Interactions on the Vibrational Energy Relaxation Dynamics of Large Molecules in Liquids. *J. Phys. Chem. A* **2007**, *111*, 6135–6145.

(47) Kovalenko, S. A.; Schanz, R.; Hennig, H.; Ernsting, N. P. Cooling Dynamics of an Optically Excited Molecular Probe in Solution from Femtosecond Broadband Transient Absorption Spectroscopy. *J. Chem. Phys.* **2001**, *115*, 3256–3274.

(48) Lower, S. K.; El-Sayed, M. A. The Triplet State and Molecular Electronic Processes in Organic Molecules. *Chem. Rev.* **1966**, *66*, 199–241.